

The Role and Detectability of the Charm Contribution to Ultra High Energy Neutrino Fluxes

Raj Gandhi^{1*}, Abhijit Samanta^{1†}, Atsushi Watanabe^{1,2‡}

¹*Harish-Chandra Research Institute, Chhatnag Road, Jhansi, Allahabad -211019, India*

²*Department of Physics, Kyushu University, Fukuoka 812-8581, Japan*

(May, 2009)

Abstract

It is widely believed that charm meson production and decay may play an important role in high energy astrophysical sources of neutrinos, especially those that are baryon-rich, providing an environment conducive to pp interactions. Using slow-jet supernovae (SJS) as an example of such a source, we study the detectability of high-energy neutrinos, paying particular attention to those produced from charmed-mesons. We highlight important distinguishing features in the ultra-high energy neutrino flux which would act as markers for the role of charm in the source. In particular, charm leads to significant event rates at higher energies, after the conventional (π , K) neutrino fluxes fall off. We calculate event rates both for a nearby single source and for diffuse SJS fluxes for an IceCube-like detector. By comparing muon event rates for the conventional and prompt fluxes in different energy bins, we demonstrate the striking energy dependence in the rates induced by the presence of charm. We also show that it leads to an energy dependant flux ratio of shower to muon events, providing an additional important diagnostic tool for the presence of prompt neutrinos. Motivated by the infusion of high energy anti-electron neutrinos into the flux by charm decay, we also study the detectability of the Glashow resonance due to these sources.

*raj@hri.res.in

†abhijit@hri.res.in

‡watanabe@hri.res.in/watanabe@higgs.phys.kyushu-u.ac.jp

1 Introduction

Over the coming decade, the detection of cosmic neutrinos is both an exciting prospect and a challenge. The considerable efforts deployed towards its realization are made worthwhile by the potential to add to our knowledge, both of the astrophysics of high energy sources and of physics beyond the standard model [1]. The extant and forthcoming km^3 sized facilities [2, 3, 4] may detect high-energy neutrinos from sources such as Active Galactic Nuclei (AGN) and Gamma Ray Bursts (GRB), heralding a new chapter in neutrino physics. Specifically, if such neutrinos are observed, their intensity and spectrum would provide key information towards understanding the dynamics of their source objects. They may also shed light on the origin of the observed cosmic rays. Additionally, flavor ratios for the three types of neutrinos may provide insights into new physics beyond the standard model, e.g., neutrino decay, the presence of pseudo-Dirac mass states and CPT violation [5, 6, 7]. The expected flux ratio $\Phi_e : \Phi_\mu : \Phi_\tau = 1 : 2 : 0$ in many sources is very sensitive to the existence of these effects. If a significant deviation from the resulting democratic distribution $\Phi_e : \Phi_\mu : \Phi_\tau = 1 : 1 : 1$ expected at earth-based detectors (after oscillation effects are incorporated) [8] is reconstructed from the observations, it would be a clear signal of new physics.

An unresolved issue which is expected to significantly affect the emitted and observed neutrino fluxes and their ratios is the role played by charm meson production and subsequent decay. Such mesons are significantly short-lived compared to π and K mesons, which are copiously produced in the $p\gamma$ and pp interactions which typify almost all such sources. This results in the charm meson neutrino spectrum in high energy astrophysical sources having qualitatively different features. Specifically, their decay is expected to lead to relatively flatter and elongated neutrino spectra compared to the sharply dropping contribution from π and K decays. This leads to an enhancement of higher energy neutrinos in sources where charm plays a role, as shown recently in [9]. Ratios of fluxes, which as stated above, are important diagnostics of new physics, would also be altered, since charm decay produces equal numbers of muon and electron neutrinos and antineutrinos.

While these effects may not be important in all high energy sources, they could significantly alter the observed neutrino fluxes for a class of sources which are characterized by proton rich jets, or, in general, an environment which renders pp interactions important. It is our intent in this paper to examine the observational consequences for ultra high energy detectors for this class of sources, where charm mesons are produced in significant numbers, along with π and K . Our aim is to bring out general qualitative differences which would stand out as markers for the presence of charm production via pp interactions in the source. If observed, this would also shed light on the issue of the presence and relative importance of pp interactions versus $p\gamma$ interactions.

As a specific case in point, to facilitate quantitative estimates of event rates from which conclusions may be drawn, we choose as source slow-jet supernovae (SJS), which have been the focus of recent studies [9, 10, 11]. However, several important features related to observations which emerge from our calculations for SJS may be generic to other types of sources whose jets are baryon rich.

To this end, we calculate the event rates using the fluxes given in [9, 10, 11]. This is done both for a single SJS source and for the diffuse flux obtained by summing over sources. While it was shown in [10, 11] that a nearby source (at around 3 Mpc) is

observable via its neutrinos from π and K decay, we show that the charm, or prompt component adds substantially to the neutrino event rate at energies significantly above those spanned by the conventional flux. Additionally, we find that due to the charmed-meson contribution, the diffuse flux from SJS alone can rise above the atmospheric neutrino background, and may already be constrained by the AMANDA observations [2]. It must be noted, however, that flux estimates of high energy sources, though usually underpinned by reliable physics, have inherent uncertainties. This is more so in the case of charm contributions, with their added QCD-related uncertainty. The event numbers we compute are intended to serve as estimates, whereas the qualitative observational features which are pointed out here, distinguishing the presence of charm contributions, may, in the long run, serve as more useful diagnostic tools as experiments accumulate data over the next decade.

The plan of the paper is as follows: In Section 2, we briefly review the physics of SJS supplemented by charm meson production. We discuss the qualitative features of the flux and, for practical use, give its fitting functions. We then calculate the event rates and spectrum in an IceCube-like detector. In Section 3, we obtain the diffuse flux and associated event rate by summing up all contributions from SJS point sources. Section 4 is devoted to a discussion of our results and conclusions.

2 Neutrinos from Slow-Jet Supernovae

2.1 The neutrino flux

Since the discovery of the connections between long duration GRB and supernovae [12], it has been conjectured that a significant fraction of core-collapse supernovae (SNe) may be accompanied by mildly relativistic jets which do not break through the stellar envelope. The choked jet may give rise to a radio after-glow without prompt γ ray signals, and such objects may be detectable primarily only via their neutrino emission. The neutrino spectrum resulting from this scenario was first modeled by Razzaque, Mészáros, and Waxman (RMW) [10] and extended by Ando and Beacom (AB) [11]. The essential difference between SJS and the related GRB jets is the mild gamma factor of the former, $\Gamma \simeq 3$ and its baryon rich environment which makes pp collisions efficient.

An extension of the work in [10, 11] has recently been discussed in [9]. These authors calculate the neutrino flux from charm meson production and decay in the source, by solving the cascade equations which describe the propagation of protons and mesons. The proton rich environment inside the slow jets is naturally conducive to charm production via pp interactions. Daughter neutrinos from charmed mesons typically have energies higher than those resulting from conventional ones. These mesons decay quickly, producing $\nu_{e,\mu} + \bar{\nu}_{e,\mu}$, before significant energy loss via interactions can occur, so that their contribution to the neutrino flux becomes dominant at $\gtrsim 10^{4.5}$ GeV. This result is a significant change in the overall features of the emergent neutrino flux and, to an extent, in its flavor composition.

In general, meson spectra, whose shapes are inherited by the daughter neutrinos, are characterized by two power-law energy breaking scales. The first breaking point $E^{(1)}$ is determined by the competition between decay and hadronic cooling (the latter characterized by, for instance, πp and Kp interactions). The second energy $E^{(2)}$ is determined by the transition between hadronic cooling and radiative cooling and marks

the onset of the latter. Below the first breaking energy, meson decay is dominant and the spectrum is the same as that of the shock accelerated protons, $\sim E^{-2}$. Between the first and the second scale, hadronic cooling is dominant, and the spectrum gets steeper to $\sim E^{-3}$. Above the second breaking energy, radiative cooling dominates, and the spectrum falls as $\sim E^{-4}$ up to the cutoff given by the proton maximal energy. For pions, the two breaking energies are close to each other and relatively low; $E^{(1)} \sim 30$ GeV and $E^{(2)} \sim 100$ GeV. Thus the pion flux retains an E^{-4} power over TeV scales, up to the maximal cutoff energy. For kaons, the relevant breaking energies are given by $E^{(1)} \sim 0.2$ TeV and $E^{(2)} \sim 20$ TeV [11].

For the charmed mesons D^\pm and D^0 , due to their short lifetimes and large masses, the two scales are close to each other and have relatively high values, $E^{(1)} \sim E^{(2)} \sim 10^4$ TeV [9]. Thus the charmed flux maintains a E^{-2} power law all the way up to the proton maximal energy, leading to a significantly flatter spectrum.

In Fig. 1, we show various fluxes of muon neutrinos and antineutrinos at an Earth detector. The calculation uses RMW [10], AB [11] and ERS [9] source fluxes and propagates them to the earth for an assumed SJS source at a distance of 20 Mpc. The fluxes are shown without neutrino oscillation effects, which we discuss in a later sub-section. We note that the flux estimates for muon neutrinos from π and K differ in the three models, while exhibiting similar spectral shapes. The differences, in part, result from differing treatments of the maximal proton cutoff energies.

For the ERS case, we also show the flux resulting from the incorporation of D^\pm -meson flux (The curve for D^0 is similar to that for D^\pm). We note that the ERS- D flux becomes dominant above $E_\nu \sim 10^5$ GeV. This flux, after propagation over a distance d_L from the source at redshift z is well represented by the following fitting function,

$$F_D = \frac{L_{\text{eff}}^D}{2\pi d_L^2} \cdot \frac{(1+z)}{E_\nu^2} \cdot \exp \left[- \left(\frac{(1+z)E_\nu}{E_{\text{br}}^D} \right)^{\beta_D} \right], \quad (2.1)$$

where

$$L_{\text{eff}}^D = 2.6 \times 10^{50} \text{ GeV} \cdot \text{s}^{-1}, \quad (2.2)$$

$$E_{\text{br}}^D = 10^{6.5} \text{ GeV}, \quad (2.3)$$

$$\beta_D = 1.35. \quad (2.4)$$

Similarly, for the conventional ERS ($\pi + K$ meson) flux, we find

$$F_C = \frac{L_{\text{eff}}^C}{2\pi d_L^2} \cdot \frac{(1+z)}{E_\nu^2} \cdot \left(\frac{(1+z)E_\nu}{E_{\text{br}}^C} \right)^{-\beta_C}, \quad (2.5)$$

where

$$L_{\text{eff}}^C = 3.1 \times 10^{50} \text{ GeV} \cdot \text{s}^{-1}, \quad (2.6)$$

$$E_{\text{br}}^C = 10^{4.5} \text{ GeV}, \quad (2.7)$$

$$\beta_C = \begin{cases} 1.0 & \text{for } E_\nu < E_{\text{br}}^C, \\ 2.2 & \text{for } E_\nu > E_{\text{br}}^C. \end{cases} \quad (2.8)$$

These expressions are useful not only for calculating the event numbers but also to deduce the diffuse flux, both of which we discuss below. The above fluxes do not

accommodate the effect of the meson accelerations by the internal shock [13]. We note, however, that accounting for this acceleration and subsequent losses due to the increased lifetime and increased interactions would lower the ERS flux estimates, and the event rate predictions we make in this paper for them.

2.2 Neutrino oscillation effects

The neutrinos produced at a source can change flavors during propagation to earth. Although their energies are very high, the distance between a source and a detector is also large enough to average out the oscillatory behavior. Writing the vacuum transition probabilities between flavor eigenstates α and β in terms of the lepton mixing matrix V only, we have [8]

$$\begin{aligned} P_{\alpha\beta} &= |V_{\alpha i}|^2 |V_{\beta i}|^2 \\ &\simeq \begin{pmatrix} 1-2s & s & s \\ s & \frac{1}{2}(1-s) & \frac{1}{2}(1-s) \\ s & \frac{1}{2}(1-s) & \frac{1}{2}(1-s) \end{pmatrix}, \end{aligned} \quad (2.9)$$

where $s \equiv \cos^2 \theta_{12} \sin^2 \theta_{12}$ and θ_{12} is the solar angle in the standard parameterization for V . The simple form of Eq. (2.9) is a result of setting the ‘‘reactor’’ and ‘‘atmospheric’’ mixing angles as $\theta_{13} = 0^\circ$ and $\theta_{23} = 45^\circ$ respectively. As a consequence of this maximal μ - τ mixing, the flux ratio of Φ_μ and Φ_τ at earth must be 1. In addition, the standard ratio $\Phi_e : \Phi_\mu : \Phi_\tau = 1 : 2 : 0$ at a source means results in a democratic configuration $\Phi_e : \Phi_\mu : \Phi_\tau = 1 : 1 : 1$ at a detector, independent of the value of θ_{12} .

For SJS, the environment is baryon rich and muons lose their energy before decaying. Thus, for the pion and kaon fluxes, the initial configurations are $\Phi_e : \Phi_\mu : \Phi_\tau = 0 : 1 : 0$. On the other hand, charmed mesons decay semi-leptonically such that the initial ratio is $\Phi_e : \Phi_\mu : \Phi_\tau = 1 : 1 : 0$. According to Eq. (2.9), these initial fluxes at the source will be transmuted to $P \cdot (0, 1, 0)^T = (s, (1-s)/2, (1-s)/2)^T = (0.22, 0.39, 0.39)^T$ and $P \cdot (1, 1, 0)^T = (1-s, (1+s)/2, (1+s)/2)^T = (0.78, 0.61, 0.61)^T$ at earth, where we have used $\theta_{12} = 34.5^\circ$ as a current best fit value [14]. To summarize, we note the fluxes Eq. (2.1) and Eq. (2.5) after oscillation are given by $F_C^e = s \cdot F_C$, $F_D^e = (1-s) \cdot F_D$, $F_C^\mu = (1-s)/2 \cdot F_C$, and $F_D^\mu = (1+s)/2 \cdot F_D$, denoting the flavor species by upper subscripts.

The difference of the initial flavor ratio between the prompt and the conventional fluxes and their different spectral behavior gives rise to an energy dependent flavor ratio at earth. This is given by

$$\frac{\Phi_e}{\Phi_\mu} = 2 \frac{s \Phi_C + (1-s) \Phi_D}{(1-s) \Phi_C + (1+s) \Phi_D}, \quad (2.10)$$

where $\Phi_{C,D}$ stand for generic charm and conventional fluxes. The ratio is bounded as follows, $2s/(1-s) \approx 0.56 < \Phi_e/\Phi_\mu < 2(1-s)/(1+s) \approx 1.28$ by the high and low-energy asymptotic behavior, marked by the dominance of the prompt and the conventional component respectively. The energy dependence is most significant around the energy at which the prompt and conventional components are equal. We show the behavior of the ratio Eq. (2.10) by the solid curve in Fig. 2, by plotting the prompt and conventional flux Eq. (2.1) and Eq. (2.5) at $d_L = 20$ Mpc. Of course, this remains unaltered when we compute the diffuse flux by integrating over the distribution and luminosity of sources,

	$10^{3\sim 4}$	$10^{4\sim 5}$	$10^{5\sim 6}$	$10^{6\sim 7}$	$10^{7\sim 8}$	Total
ERS- $D^{\pm,0}$	37	90	40	4	0	171
ERS- K, π	107	39	0.4	0	0	146
AB- K, π	3	1	0	0	0	4
RMW- K, π	7	3	0	0	0	10

Table 1: The number of up-going $\nu_\mu N \rightarrow \mu X$ events from an SJS at 3 Mpc. The columns show the events in each decade of energy (in GeV) and the total events. An instrumented volume of $V = 1(\text{km}^3)$, and an energy threshold $E_\mu^{\text{min}} = 10^3$ (GeV) is assumed.

since it depends only on the mixing matrix and the fact that the oscillation length is much shorter than the source distance.

Fig. 2 highlights the importance of detecting both electron and muon flavored neutrinos, particularly in the high-energy region above 50 TeV. The rise of the ratio above unity at high-energy will be an indication that charmed mesons contribute to neutrino production. In addition, the observation of the transition of the ratio around $1 \sim 100$ TeV would indicate that the source environments are baryon rich, to a degree that allows the charm component to rise above the conventional π, K component and the muon to be damped. We also note the significant difference in the SJS without charm and SJS with charm curves in the figure, i.e from a constant 0.5 for the former, to an energy dependant transition from 0.5 to 1.25 for the latter. Thus, shower events would register an increase from their low values compared to muon events at low energies, and rise above them at high energies.

We note that the canonical flavor ratio $\Phi_e : \Phi_\mu : \Phi_\tau = 1 : 2 : 0$, the ratio for muon damped sources, $\Phi_e : \Phi_\mu : \Phi_\tau = 0 : 1 : 0$ and that for semi-leptonic D decay, $\Phi_e : \Phi_\mu : \Phi_\tau = 1 : 1 : 0$ should all be regarded as idealizations which can be used as first approximations. More precisely, there can be small deviations from the above standard ratios with some uncertainties [15]. For example, it has been discussed that the muon damping cannot be perfect and ν_e component consequently never can fall to zero [15]. Inclusion of these effects will amount to finite thickness for the curves presented in Fig. 2. However, qualitative behavior such as the transition of the ratio around $1 \sim 100$ TeV will not change significantly and the curves in Fig. 2 still represent the essential qualitative physics of the charm effect.

2.3 Detection of high-energy neutrinos

We next compute the up and down-going event rates for an IceCube-like detector for the fluxes considered in the previous sub-section, assuming a point source at a distance of 3 Mpc. While this has been previously done in [10, 11] for the conventional flux, our purpose here is to compare this contribution quantitatively with that of the charm mesons.

For up-going events, we incorporate the attenuation of neutrino flux by the earth matter, and also consider partially contained events which enhance the effective volume of the detector significantly for muon events. The event rate is given by [16]

$$\text{Rate} = AN_A \int dE_\nu \cdot \langle R(E_\mu^{\text{min}}, E_\nu) \rangle \cdot \sigma_{CC}(E_\nu) \cdot S(E_\nu) \cdot F_{C,D}^\mu \quad (2.11)$$

	$10^{3\sim 4}$	$10^{4\sim 5}$	$10^{5\sim 6}$	$10^{6\sim 7}$	$10^{7\sim 8}$	Total
ERS- $D^{\pm,0}$	44	26	9	1.3	0	80
ERS- K, π	228	13	0.1	0	0	241
AB- K, π	7	0.3	0	0	0	7
RMW- K, π	17	1	0	0	0	18

Table 2: Same as Table 1, but for down-going $\nu_\mu N \rightarrow \mu X$ events.

where A is the effective area of the detector, and N_A is Avogadro's number $N_A = 6.022 \times 10^{23} \text{ (cm}^{-3}\text{)}$. The muon range $\langle R(E_\mu^{\text{min}}, E_\nu) \rangle$ stands for the average distance traversed by a muon in earth matter. Muons created by neutrinos with energy E_ν attenuate to the energy E_μ^{min} , after traveling $\langle R(E_\mu^{\text{min}}, E_\nu) \rangle$. The factor $S(E_\nu)$ represents the shadowing (i.e attenuation) of the up-going neutrinos by the earth.

For down-going events, the event rate for the $\nu N \rightarrow \mu X$ process is given by

$$\text{Rate} = N_A V_{\text{eff}} \int dE_\nu \cdot \sigma_{CC}(E_\nu) \cdot F_{C,D}^\mu \quad (2.12)$$

where V_{eff} is the effective volume of the detector, assumed here to be $1 \text{ (km}^3\text{)}$. σ_{CC} is the neutrino-nucleon charged current cross section.

In addition to the $\nu N \rightarrow \mu X$ events, we have also calculated events for the Glashow resonance process, $\bar{\nu}_e e \rightarrow \text{something}$, which peaks around $E_\nu = 6.3 \text{ PeV}$, primarily because we expect an enhanced contribution from charm at the higher energies. The event rate for down-moving neutrinos from this channel is given by

$$\text{Rate} = \frac{10}{18} N_A V_{\text{eff}} \int dE_\nu \cdot \sigma_{\bar{\nu}_e e}(E_\nu) \cdot \frac{1}{2} F_{C,D}^e \quad (2.13)$$

Our results for all the various event spectra are shown in Fig. 3(4) for up(down)-going events. Clearly, the charm contribution dominates above $\sim 50 \text{ TeV}$, and its contribution is significant even around $500 - 1000 \text{ TeV}$, where the π and K contributions to the event rate are negligible. Table 1(2) shows the integrated number of events for each energy decade with up(down)-going muon events. First, we note that the ERS flux, even for the conventional case, yields rates which are about 20-30 times higher than the AB or RMW fluxes, due to an enhanced pp contribution in this model. The charm contribution for ERS is a full third of the integrated rate for the conventional flux. Importantly, it manifests itself in energy regions where the conventional contribution is low, i.e., in the band $10^4 - 10^6 \text{ GeV}$. This both enhances its prospects for detection and acts as a distinctive signature for charm. Finally, we note that since the typical duration of the burst is a few seconds, the background from the atmospheric flux is small.

In Fig. 4, we show the event spectrum for $\bar{\nu}_e e \rightarrow \bar{\nu}_\mu \mu$ channel as well. From the figure, we can clearly see the resonant behavior at 6.3 PeV . The number of events for this mode is, with the ERS- D flux, 0.06 in the $10^{5\sim 6} \text{ GeV}$ bin. While this contribution is $\sim 50 \%$ of its total event tally over the full energy range of $10^{3\sim 8} \text{ GeV}$, it is unfortunately too tiny to be detectable.

3 The Diffuse neutrino flux from SJS

3.1 The diffuse neutrino flux

Prior to presenting our results for the events from the diffuse SJS fluxes, we note that charm is likely to contribute to the atmospheric flux as well. This has been discussed in detail in, for example, in [17]. We have ascertained that its contribution is low and does not constitute a significant background to the SJS flux.

The diffuse neutrino flux is obtained by integrating the point source flux over all SNe, weighting the flux by a rate $\frac{d^2 N_{\text{sn}}}{dt d\Omega}$, the number of SNe events per unit time per solid angle covering the earth sky. The distribution $\frac{d^2 N_{\text{sn}}}{dt d\Omega}$ is given by [10]

$$\frac{d^2 N_{\text{sn}}}{dt d\Omega} = \frac{\dot{n}_{\text{sn}}(z) d_L^2 c}{(1+z)^2} \left| \frac{dt}{dz} \right|, \quad (3.1)$$

where the SNe rate $\dot{n}_{\text{sn}}(z)$ is

$$\dot{n}_{\text{sn}}(z) = 0.017 \frac{0.32 e^{3.4z}}{e^{3.8z} + 45} \times 10^{-81} \quad (\text{s}^{-1} \cdot \text{cm}^{-3}). \quad (3.2)$$

The cosmic time t and z is related as

$$\left| \frac{dt}{dz} \right| = \frac{1}{H_0} \frac{1}{1+z} \frac{1}{\sqrt{(1+\Omega_m z)(1+z)^2 - \Omega_\Lambda(2z+z^2)}}, \quad (3.3)$$

where $\Omega_m = 0.3$ and $\Omega_\Lambda = 0.7$ within the standard cosmology. With these ingredients at hand, the diffuse neutrino flux is given by (e.g. for charm flux)

$$\begin{aligned} \Phi_D^{\text{diff}} &= \frac{\xi_{\text{sn}}}{2\Gamma^2} \int_0^\infty dz \cdot \frac{d^2 N_{\text{sn}}}{dt d\Omega} \cdot t_j F_D^\mu \\ &= \frac{\xi_{\text{sn}}}{4\pi\Gamma^2} \cdot \frac{c L_{\text{eff}}^D t_j}{E_\nu^2} \int_0^\infty dz \cdot \frac{\dot{n}_{\text{sn}}(z)}{(1+z)} \left| \frac{dt}{dz} \right| \exp \left[- \left(\frac{(1+z) E_\nu}{E_{\text{br}}^D} \right)^{\beta_D} \right], \end{aligned} \quad (3.4)$$

where t_j is the jet duration of $\simeq 10$ s, and ξ_{sn} represents a rate of SNe with an accompanying jet. The probability that the jet points to the earth is assumed to be $1/2\Gamma^2$.

In Fig. 5, we show $\nu_\mu + \bar{\nu}_\mu$ diffuse fluxes. From the figure, we can see that the total contribution for the ERS flux already begins to breach AMANDA data, and hence the charm contribution is likely to be both tested and constrained over the coming years. As already pointed out, the range over which it is dominant is largely different from that spanned by the conventional contribution from π and K mesons, making it observationally distinct.

Table 3 shows the number of the events per year per steradian for each flux. In Fig. 5 and Table 3, we have, somewhat unrealistically, endowed all supernovae with slow jets of $\Gamma = 3$, and thus taken $\xi_{\text{sn}} = 1$. For the ERS fluxes, the diffuse rates are quite high and certainly observable, especially in the higher background free energy bins. Roughly, a total of 200 up-going and 180 down-going events are expected per year[§]. A more realistic value of ξ_{sn} would lower our rates by an appropriate factor.

[§] We note that the Waxman-Bahcall bound [18], which appears to be breached, does not apply to such sources since they do not contribute to the cosmic-ray flux

	$10^{3\sim 4}$	$10^{4\sim 5}$	$10^{5\sim 6}$	$10^{6\sim 7}$	$10^{7\sim 8}$	Total
ERS- $D^{\pm,0}$	34	82	36	4	0	156
ERS- K, π	45	16	0	0	0	61
AB- K, π	0.7	0.2	0	0	0	1
RMW- K, π	2	0.5	0	0	0	3

Table 3: The number of up-going muon events per year per steradian with the diffuse prompt and conventional fluxes. The instrumented volume of the detector is taken as $V = 1$ (km³); the effective area $A = 1$ (km²) for up-going and the effective volume $V_{\text{eff}} = 1$ (km³) for down-going. We are taking the energy threshold as $E_{\mu}^{\text{min}} = 10^3$ (GeV).

	$10^{3\sim 4}$	$10^{4\sim 5}$	$10^{5\sim 6}$	$10^{6\sim 7}$	$10^{7\sim 8}$	Total
ERS- $D^{\pm,0}$	40	24	8	1	0	73
ERS- K, π	98	5	0	0	0	103
AB- K, π	1	0	0	0	0	1
RMW- K, π	4	0.2	0	0	0	4

Table 4: Same as Table 3, but for down-going muon events.

Finally, we present simple fits to the flux curves for the muon neutrinos shown in Fig. 5. The fluxes are well represented by

$$y = ax^b + ce^{dx}, \quad (3.5)$$

where $y = \log_{10}(\Phi E_{\nu}^2)$, $x = \log_{10}(E_{\nu})$. The diffuse flux Φ and the neutrino energy E_{ν} are in the same units as in Fig. 5. Using Eq. (3.5), the neutrino flux for each case, (i) SJS conventional (ii) SJS D -meson and (iii) SJS total can be fitted and the sets of the best-fit parameters, a, b, c , and d are listed in Table 5.

4 Summary and Conclusion

The production and decay of charmed mesons can play an important role for the detection of high-energy cosmic neutrinos. Slow-jet supernovae provide both an excellent example and a test case in which the charm effect can be significant due to the baryon rich environment, leading to the rise of pp contributions to the total neutrino rate. This enhances the detectability of the SJS neutrinos not only with the point sources but also with the diffuse flux.

The charm contribution appears to open up the possibility of detecting SJS via their diffuse flux, using the ERS flux calculations. While the absolute intensity of the flux should be regarded with caution at the present stage, the elongated shape of the total flux offers a shot at detection, provided pp interactions play a significant role, and if the jet parameters (and the fraction ξ_{sn}) are favorable.

By virtue of the semileptonic decay of the charmed mesons, the flavor ratio Φ_e/Φ_{μ} must be $\simeq 2(1 - \sin^2\theta_{12})$, which is essentially different from the typical AGN or GRB case. Furthermore, the energy dependence of Φ_e/Φ_{μ} also carries potentially important

	a	b	c	d
(i) SJS conventional	-0.86203	1.41904	-25.73761	-0.84254
(ii) SJS D -meson	-6.20429	0.06759	-6.8552×10^{-9}	2.83302
(iii) SJS total	-5.17119	0.16516	-2.1531×10^{-8}	2.68061

Table 5: Best-fitted values of the parameters a , b , c , d for different SJS fluxes.

information. The ratio shifts occurs around the crossing point E_{cross} where the D -meson flux becomes equal to the kaon flux. The crossing energy is written as $E_{\text{cross}} \sim (f_K/f_D)E_K^{(1)} \approx 200E_K^{(1)}$, where $f_K(f_D) \simeq 0.06(3 \times 10^{-4})$ are the kaon and the charmed-meson multiplicities, and $E_K^{(1)}$ is the first breaking energy for kaon. The breaking energy $E_K^{(1)}$ is very sensitive to the bulk Lorentz factor Γ such that $E_K^{(1)} \propto \Gamma^{7 \div 5}$ depending on the assumption on the jet-opening angle [11].

To summarize, charmed mesons can play an important role in a certain class of high energy sources in general and some supernovae in particular, where jets are mildly relativistic and environments baryon-rich. Detection of the charm related neutrino flux may be possible with current and near-future detector sensitivities, and can offer a valuable handle on several important open questions related to the dynamics of such sources.

Acknowledgments

The authors acknowledge support from the Neutrino Project under the XIth plan of Harish-Chandra Research Institute, and thank Mary Hall Reno and Rikard Enberg for useful discussions.

References

- [1] F. Halzen, J. Phys. Conf. Ser. **120**, 062004 (2008) [arXiv:0710.4158 [astro-ph]]; C. Quigg, arXiv:0802.0013 [hep-ph]; N. F. Bell, J. Phys. Conf. Ser. **136**, 022043 (2008) [arXiv:0811.0847 [astro-ph]].
- [2] J. Ahrens *et al.* [AMANDA Collaboration], Phys. Rev. D **66**, 012005 (2002) [arXiv:astro-ph/0205109]; A. Achterberg *et al.* [IceCube Collaboration], arXiv:astro-ph/0509330.
- [3] J. Ahrens *et al.* [IceCube Collaboration], Astropart. Phys. **20**, 507 (2004) [arXiv:astro-ph/0305196].
- [4] U. F. Katz, Nucl. Instrum. Meth. A **567**, 457 (2006) [arXiv:astro-ph/0606068].
- [5] J. F. Beacom, N. F. Bell, D. Hooper, S. Pakvasa and T. J. Weiler, Phys. Rev. Lett. **90**, 181301 (2003) [arXiv:hep-ph/0211305]; Phys. Rev. D **68**, 093005 (2003) [Erratum-ibid. D **72**, 019901 (2005)] [arXiv:hep-ph/0307025]; S. Pakvasa, Mod. Phys. Lett. A **19**, 1163 (2004) [Yad. Fiz. **67**, 1179 (2004)] [arXiv:hep-ph/0405179].

- [6] J. F. Beacom, N. F. Bell, D. Hooper, J. G. Learned, S. Pakvasa and T. J. Weiler, Phys. Rev. Lett. **92**, 011101 (2004) [arXiv:hep-ph/0307151]; P. Keranen, J. Maalampi, M. Myyrylainen and J. Riittinen, Phys. Lett. B **574**, 162 (2003) [arXiv:hep-ph/0307041].
- [7] G. Barenboim and C. Quigg, Phys. Rev. D **67**, 073024 (2003) [arXiv:hep-ph/0301220].
- [8] H. Athar, M. Jezabek and O. Yasuda, Phys. Rev. D **62**, 103007 (2000) [arXiv:hep-ph/0005104]; C. Quigg in [1].
- [9] R. Enberg, M. H. Reno and I. Sarcevic, Phys. Rev. D **79**, 053006 (2009) [arXiv:0808.2807 [astro-ph]].
- [10] S. Razzaque, P. Meszaros and E. Waxman, Phys. Rev. Lett. **93**, 181101 (2004) [Erratum-ibid. **94**, 109903 (2005)] [arXiv:astro-ph/0407064]; Mod. Phys. Lett. A **20**, 2351 (2005) [arXiv:astro-ph/0509729].
- [11] S. Ando and J. F. Beacom, Phys. Rev. Lett. **95**, 061103 (2005) [arXiv:astro-ph/0502521].
- [12] J. Hjorth *et al.*, Nature **423**, 847 (2003) [arXiv:astro-ph/0306347]; K. Z. Stanek *et al.*, Astrophys. J. **591**, L17 (2003) [arXiv:astro-ph/0304173].
- [13] H. B. J. Koers and R. A. M. Wijers, arXiv:0711.4791 [astro-ph].
- [14] M. Maltoni, T. Schwetz, M. A. Tortola and J. W. F. Valle, New J. Phys. **6**, 122 (2004) [arXiv:hep-ph/0405172], version 6.
- [15] M. Kachelriess and R. Tomas, Phys. Rev. D **74**, 063009 (2006) [arXiv:astro-ph/0606406]; P. Lipari, M. Lusignoli and D. Meloni, Phys. Rev. D **75**, 123005 (2007) [arXiv:0704.0718 [astro-ph]]; S. Pakvasa, W. Rodejohann and T. J. Weiler, JHEP **0802**, 005 (2008) [arXiv:0711.4517 [hep-ph]].
- [16] R. Gandhi, C. Quigg, M. H. Reno and I. Sarcevic, Astropart. Phys. **5**, 81 (1996) [arXiv:hep-ph/9512364]; Phys. Rev. D **58**, 093009 (1998) [arXiv:hep-ph/9807264].
- [17] P. Gondolo, G. Ingelman and M. Thunman, Astropart. Phys. **5**, 309 (1996) [arXiv:hep-ph/9505417]; R. Enberg, M. H. Reno and I. Sarcevic, Phys. Rev. D **78**, 043005 (2008) [arXiv:0806.0418 [hep-ph]].
- [18] E. Waxman and J. N. Bahcall, Phys. Rev. D **59**, 023002 (1999) [arXiv:hep-ph/9807282].

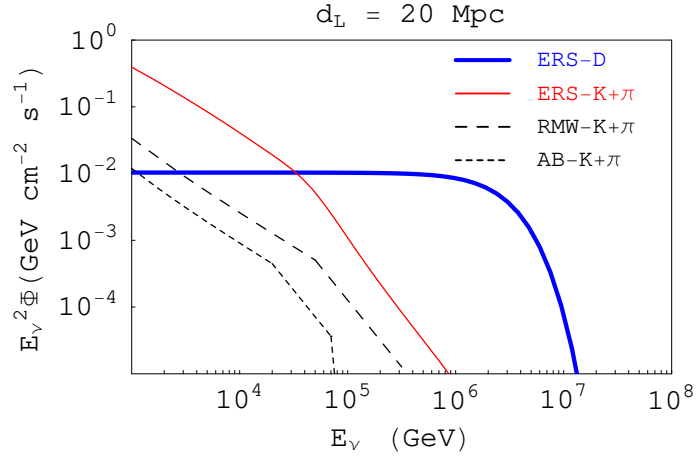


Figure 1: Muon neutrino and antineutrino fluxes from a source at 20 Mpc. The thick(thin)-solid curve shows the $D^\pm(K^\pm + \pi^\pm)$ flux in [9]. The dashed and dotted curves are the $K^\pm + \pi^\pm$ fluxes in [10] and [11] respectively. The fluxes are given in the earth-observer frame. The effects of neutrino oscillation are not incorporated in this set of curves.

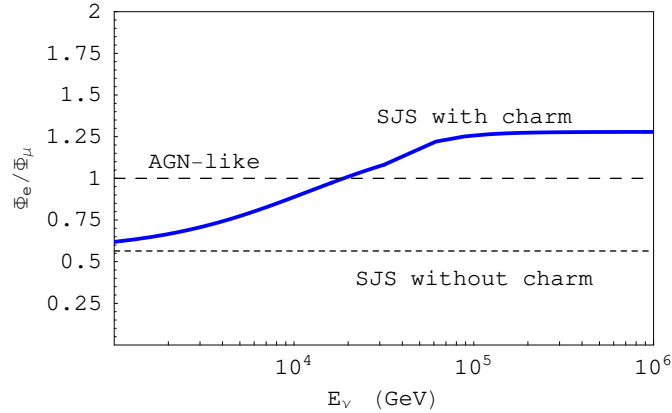


Figure 2: The e/μ flavor ratio of the flux, as a function of the neutrino energy. The solid curve shows the full contribution with SJS. The dotted line is for SJS, but only with the conventional component. The dashed line represents a typical value for the sources which allow full muon decay, such as AGN (without charm).

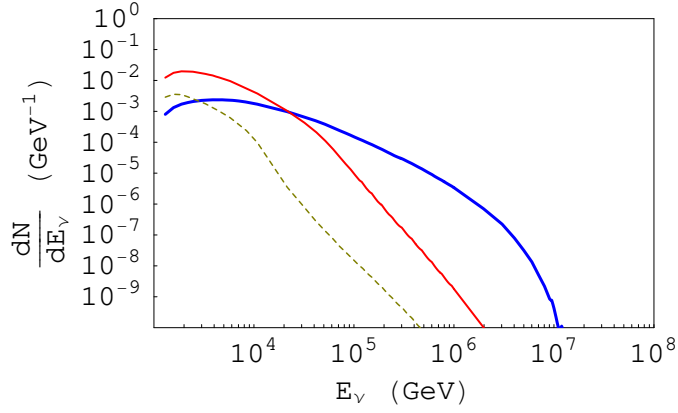


Figure 3: Event spectrum of up-going $\nu N \rightarrow \mu^- X$ with a source at $d_L = 3$ Mpc for ERS flux [9]. The blue (thick solid), red (thin solid) and the dashed curve shows D^\pm , K and π contribution respectively.

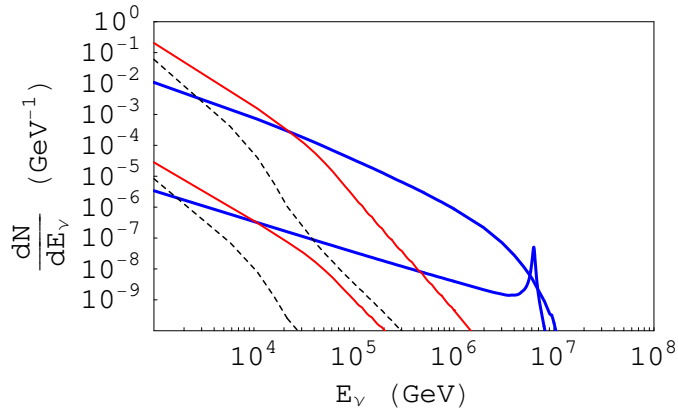


Figure 4: Same as Fig. 3 but for down-going events. The lower curve in each case is for $\bar{\nu}_e e \rightarrow \bar{\nu}_\mu \mu$ channel.

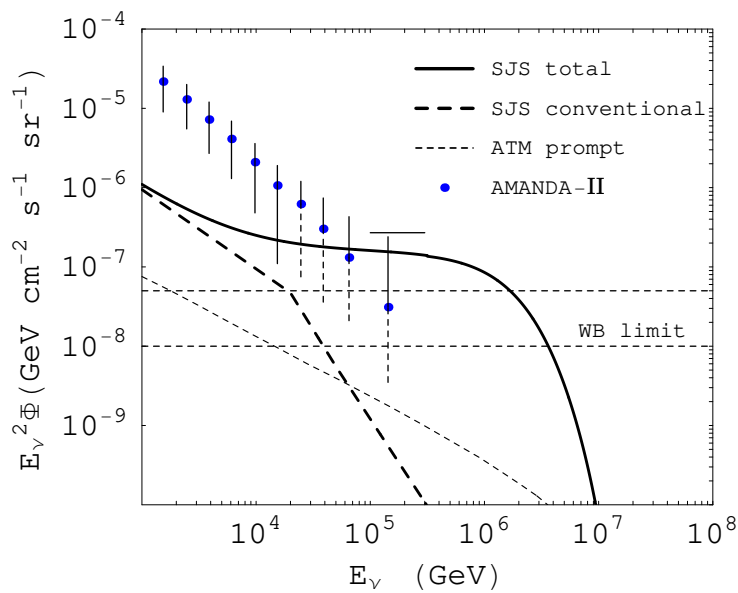


Figure 5: The diffuse $\nu_\mu + \bar{\nu}_\mu$ flux from slow-jet supernovae, compared with the reconstructed atmospheric neutrino flux by AMANDA 2000 year data [2]. The thick plain (dashed) curve shows the total (conventional) flux for SJS, and the thin dashed curve is the prompt flux from the atmosphere [17]. The horizontal dashed lines shows the WB limit $\sim 1 - 5 \times 10^{-8} \text{ GeV} \cdot \text{cm}^{-2} \cdot \text{s}^{-1} \cdot \text{sr}^{-1}$ [18].